Magnetic polarons and spin-glass behavior in insulating $La_{1-x}Sr_xCoO_3$ ($x = 0.125$ and 0.15)

P. Anil Kumar,[1,2,*] Abhishek Nag,[2,†] Roland Mathieu,[1] Ranjan Das,[3] Sugata Ray,[2] Per Nordblad,[1] Akmal Hossain,[3] Dona Cherian,[3] Diego Alba Venero,[4] Lisa DeBeer-Schmitt,[5] Olof Karis,[6] and D. D. Sarma[3]

[1]*Department of Materials Science and Engineering, Uppsala University, P.O. Box 35, SE-751 03 Uppsala, Sweden*
[2]*School of Materials Science, Indian Association for the Cultivation of Science, Kolkata 700032, India*
[3]*Solid State and Structural Chemistry Unit, Indian Institute of Science, Bengaluru 560012, India*
[4]*ISIS neutron and muon source, STFC Rutherford Appleton Laboratory, Chilton, Didcot OX11 0QX, United Kingdom*
[5]*Large Scale Structures Group, Neutron Sciences Directorate, Oak Ridge National Laboratory, Oak Ridge, Tennessee 37831, USA*
[6]*Department of Physics and Astronomy, Uppsala University, Box-516, 75120 Uppsala, Sweden*

(Received 29 June 2020; revised 22 October 2020; accepted 2 November 2020; published 8 December 2020)

The evolution of magnetic polarons in Sr doped $LaCoO_3$ ($La_{1-x}Sr_xCoO_3$) single crystal and polycrystalline samples are investigated by employing dc and ac magnetic measurement and small angle neutron scattering (SANS) techniques. The effect of magnetic field and temperature on magnetic polarons is experimentally studied for $La_{0.875}Sr_{0.125}CoO_3$ and $La_{0.85}Sr_{0.15}CoO_3$ compounds that belong to the spin glass insulating regime of the broader compositional phase diagram of this system. Langevin analyses of the isothermal magnetization curves in the notional paramagnetic regime prove the existence of magnetic polarons with large moments. The dc field superimposed ac susceptibility data and the analysis of the glassy dynamics prove that the size of polarons in 15% Sr doped crystal increase as the field is increased while the field effect is not visible in the 12.5% Sr doped crystal. A polycrystalline sample of $La_{0.85}Sr_{0.15}CoO_3$ is analyzed by SANS experiments, which confirm nonzero correlation length at temperatures far above the macroscopic ordering temperature and hence the presence of magnetic polarons.

DOI: 10.1103/PhysRevResearch.2.043344

I. INTRODUCTION

$LaCoO_3$ is one of the rare transition metal oxides which exhibit a nonmagnetic ground state due to the presence of low spin (t_{2g}^6: $S = 0$) Co ions. This is due to the crystal field splitting energy being higher than the Hund's coupling energy for the Co ion in this system. However, the sample undergoes a spin state transition to intermediate/high spin state at a higher temperature [1,2]. Further, the hole doping of the system by means of, for example, Sr substitution at the La site also leads to the formation of finite moments on each Co site and a magnetic ground state in this system. Akin to the hole/electron doped rare-earth manganites, these rare-earth cobaltite perovskites also exhibit a rich phase diagram as a function of doping and temperature [3,4]. The properties of these perovskites are influenced by extrinsic factors like chemical inhomogeneity and oxygen content. However, the cobaltite systems have not been as extensively studied as the manganites, and the effects of hole doping, magnetic interactions, etc., are still unclear in case of cobaltites.

An interesting aspect of these doped cobaltites is the experimental and theoretical observations pointing to presence of spin/magnetic polarons [5,6]. A combination of inelastic neutron scattering, electron spin resonance, and nuclear magnetic resonance measurements on the lightly hole doped system $La_{0.998}Sr_{0.002}CoO_3$, predicted that the presence of spin-state polarons is the reason for high magnetic moment in hole-doped $La_{1-x}Sr_xCoO_3$ as opposed to the nonmagnetic ground state of undoped $LaCoO_3$ [7]. Similarly, magnetic and optical spectroscopy measurements on $La_{1-x}Sr_xCoO_3$ ($x =$ 0.002, 0.005, and 0.010) indicated formation of high spin ($S =$ 10–16) polarons centered on doped holes [2]. In systems with higher Sr doping ($0.05 < x < 0.18$) it has been proposed that there exists an electronically separated phase with ferromagnetic clusters embedded in a nonferromagnetic matrix [5,8–11]. The hypothesis stems from the existence of tunnel type magnetoresistance and aging effects in the electronic transport in conjunction with the glassy magnetic state.

In the present article, we study single crystals of $La_{0.875}Sr_{0.125}CoO_3$ and $La_{0.85}Sr_{0.15}CoO_3$ by detailed ac susceptibility and dc magnetic measurement techniques. The analysis of ac susceptibility data collected with a superimposed dc field is used to determine the evolution of the size of the magnetic entities, polarons, as a function of field while the analysis of isothermal magnetization curves measured above the glass ordering temperature is used to determine the

*Present address: Seagate Technology, 1 Disc Drive, Derry, Northern Ireland, United Kingdom; Corresponding author: anil.mag@gmail.com
†Present address: Diamond Light Source, Harwell Campus, Didcot OX11 0DE, United Kingdom.

evolution of these polarons as a function of temperature. Our results suggest a growth of the magnetic polaron size with increasing magnetic field or decreasing temperature in the case of $La_{0.85}Sr_{0.15}CoO_3$. However, the field effect is negligible on the polaron size in the sample $La_{0.875}Sr_{0.125}CoO_3$ whereas the polaron size increases with decreasing temperature. Small angle neutron scattering on polycrystalline samples has been used to estimate the size of the clusters as a function of the temperature.

II. EXPERIMENTAL DETAILS

Single crystals of $La_{0.875}Sr_{0.125}CoO_3$ and $La_{0.85}Sr_{0.15}CoO_3$, hereafter referred to as Sr12.5 and Sr15, respectively, are prepared by the floating zone technique using a 4-mirror optical floating zone furnace from Crystal Systems Corporation. Polycrystalline samples of the intended composition are prepared using a solid state reaction method starting from La_2O_3, $SrCO_3$ and CoO in appropriate molar ratios. The final, phase pure, polycrystalline powders are pressed into cylindrical rods using a hydrostatic press followed by sintering at 1200 °C. Two such cylindrical rods are used as feed and seed rods for single crystal growth. Growth is carried out at a rate of 6 mm/h under continuous oxygen flow. The rotation rates of the upper and lower shafts are adjusted to obtain a stable molten zone during the growth. The phase purity is confirmed within the accuracy of x-ray diffraction technique by which any impurity phase with a volume above 2–3% should be visible. The composition and chemical homogeneity of the prepared crystals are confirmed by ICP-OES in a Perkin- Elmer spectrometer and energy dispersive electron spectroscopy spot analysis in a Zeiss LEO 440 scanning electron microscope. DC magnetic measurements and low frequency ac susceptibility measurements are performed in a Quantum Design MPMS superconducting quantum interference device magnetometer and high frequency ac susceptibility measurements are performed on a Quantum Design PPMS instrument. The small angle neutron scattering (SANS) data are recorded at the SANS2D instrument in the RAL-ISIS spallation source (UK) on a separately prepared polycrystalline $La_{0.85}Sr_{0.15}CoO_3$ (Sr15) sample in the q range of 0.004–0.668 $Å^{-1}$.

III. RESULTS AND DISCUSSION

Figures 1(a) and 1(b), respectively, present magnetic moment (M) versus temperature (T) plots for the crystals Sr15 and Sr12.5 in zero-field-cooled (ZFC) and field-cooled (FC) conditions. The ZFC curve of the sample Sr12.5 displays a sharp cusp at $T_{cusp} \sim 44$ K and the ZFC, FC curves fully merge above this temperature. On the other hand, the sample Sr15 exhibits a T_{cusp} of ∼56 K along with a weak separation between ZFC and FC curves up to ∼150 K, which is far above the cusp temperature. The persistence of this separation up to a temperature far higher than T_{cusp} may indicate the presence of minute amounts of magnetic impurities or certain inhomogeneity in the strength of magnetic interactions in the sample. Such impurities or inhomogeneities may be associated with local ordering of magnetic moments at higher temperature compared to the ordering temperature of macroscopic system.

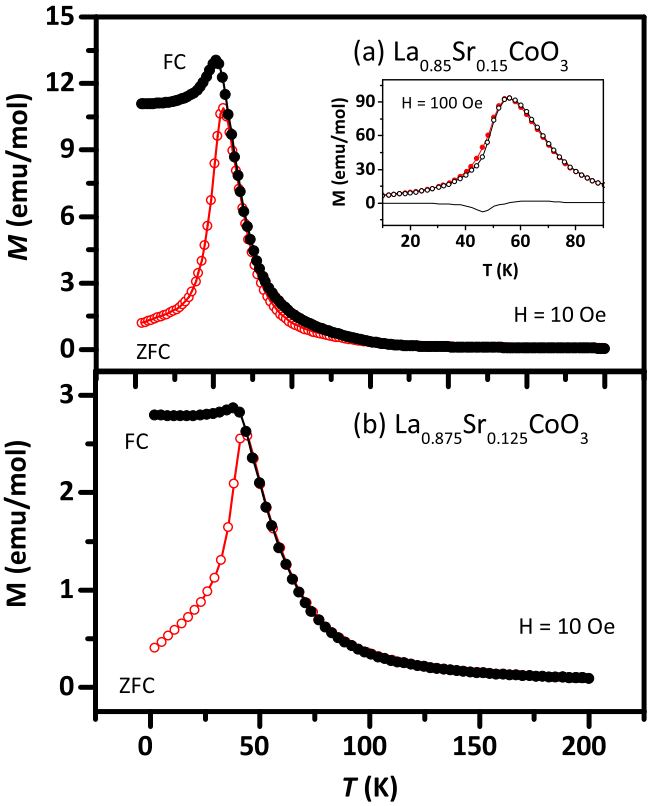

FIG. 1. The dc magnetic data collected in 10 Oe field for the crystals (a) $La_{0.85}Sr_{0.15}CoO_3$ and (b) $La_{0.875}Sr_{0.125}CoO_3$. The inset in (a) shows the results of dc memory experiment on the crystal $La_{0.85}Sr_{0.15}CoO_3$.

On the other hand, such a separation for the sample Sr12.5 disappears just above T_{cusp} making a clear distinction from the higher Sr doped sample.

It is worth noting that the sample Sr15 is closer to the reported percolation limit (∼18%) and hence such an inhomogeneity in magnetic interaction strength may be expected [8,9,12]. Figure 1(a) also shows the results of a so-called dc memory experiment as an inset [13]. For the dc memory experiment, a second ZFC M (T) curve is measured after a halt at 45 K for 3000 seconds before cooling the sample further down to 10 K and application of measuring field. The data shows a dip in the M (T) curve, close to 45 K, which is otherwise identical to the reference ZFC curve measured without any stop in cooling sequence. This dip reflects the nonequilibrium character of the underlying glassy dynamics at low temperatures [13].

We investigate the nature of the magnetic anomaly observed at T_{cusp} by using ac susceptibility measurements (Fig. 2) on these two differently doped $LaCoO_3$ compounds. The panels (a) and (c) show the real part, χ', and panels (b) and (d) show the imaginary part, χ'', of the susceptibility measured at different frequencies, f. As shown in Figs. 2(a) and 2(c), both the compositions exhibit strong frequency dependency in ac susceptibility data indicative of a glassy magnetic system. In addition, the nature of the frequency dispersion is such that the susceptibility curves measured at different frequencies tend to gradually converge below T_{cusp}.

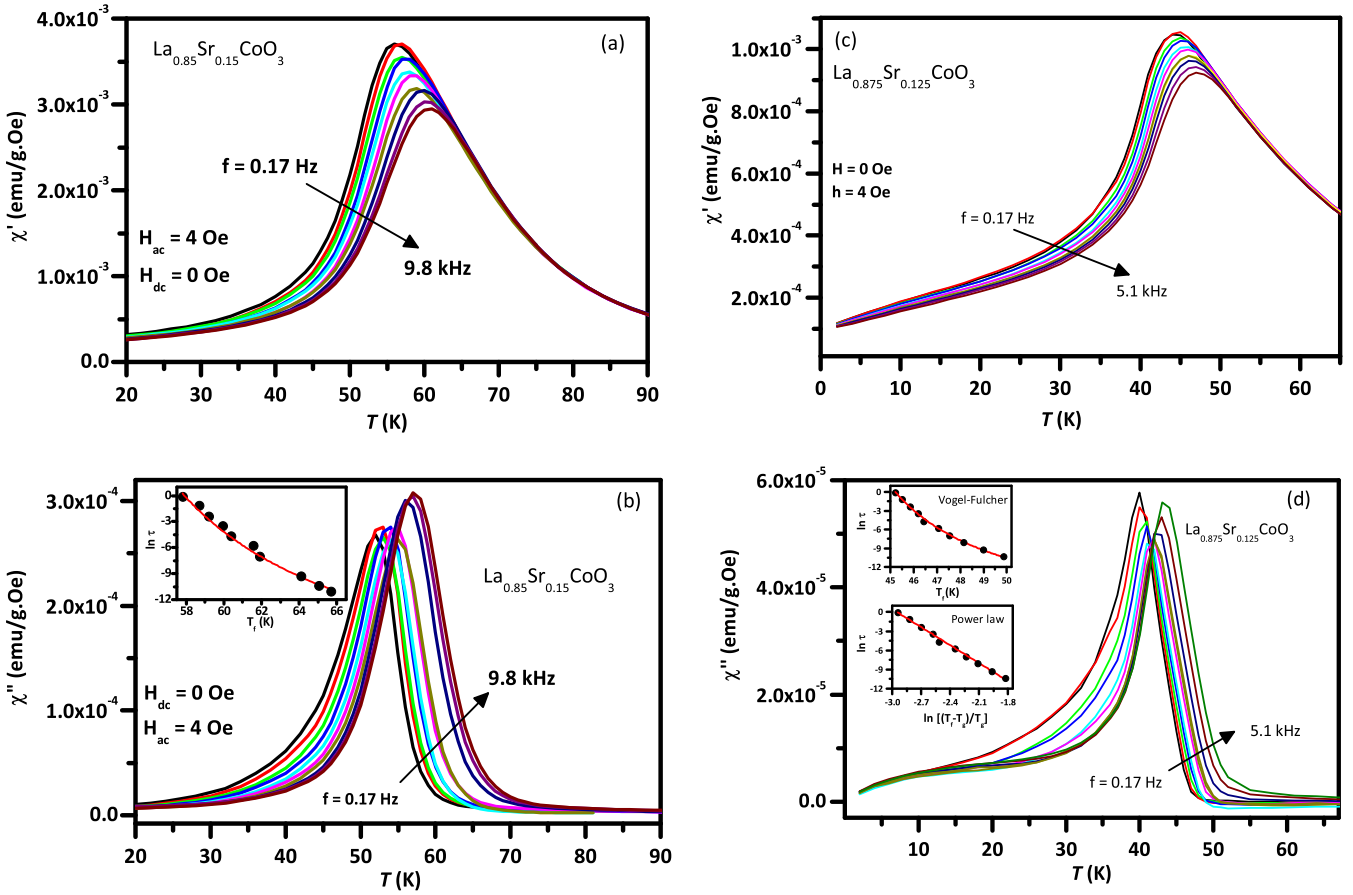

FIG. 2. The real and imaginary parts of the ac susceptibility data on sample $La_{0.85}Sr_{0.15}CoO_3$ are presented in panels (a) and (b), while the corresponding data for sample $La_{0.875}Sr_{0.125}CoO_3$ are shown in panels (c) and (d), respectively. The inset to panel (b) shows the Vogel-Fulcher fitting of $\ln\tau - T_f$ data for $La_{0.85}Sr_{0.15}CoO_3$ while the top inset to panel (d) shows the same fitting for $La_{0.875}Sr_{0.125}CoO_3$. The bottom inset of panel (d) shows the result of power law analysis for $La_{0.875}Sr_{0.125}CoO_3$. The curves correspond to 0.17, 0.51, 1.7, 5.1, 17, 51, 170, 510, 1700, 5100, and 9800 Hz.

This behavior is characteristic of a superspin glass system [14] comprising of interacting magnetic entities that are larger than the atomic spins that constitute canonical atomic spin glasses [15].

The superspin glass state in certain manganite perovskites is of the re-entrant type and the high temperature ferromagnetic state in them does not allow for a detailed analysis of the dynamics of the re-entrant superspin glass transition [16]. However, in the present case no such difficulty exists and one can do a detailed analysis of the temperature, frequency, and magnetic field dependence of the ac susceptibility to extract information on superspin glass state [17,18].

To start with, the dynamics of the two systems are determined in zero dc field and an ac field, h, of 4 Oe is used for the measurement. A frequency dependent freezing temperature T_f has been determined as the temperature at which χ'' reaches $1/6^{th}$ of its peak value as the measurement temperature is raised. The relaxation time, τ $(=1/2\pi f)$ is then fitted using the Vogel-Fulcher equation [19,20] $\tau = \tau_0 \exp(\frac{E_b}{k_B(T_f - T_0)})$ and the power law given by critical slowing down $\tau = \tau_0[\frac{T_f - T_g}{T_g}]^{-z\nu}$. The Vogel-Fulcher equation describes a system of interacting magnetic entities with E_b being the anisotropy barrier energy, T_0 is a parameter signifying the interaction strength between the magnetic entities, and τ_0 is the characteristic relaxation time [20]. On the other hand, the power law describes the dynamics of a system where a true phase transition occurs from a paramagnetic to a glassy magnetic state with a transition temperature T_g, a critical exponent $z\nu$, and characteristic relaxation time τ_0 [14]. The best possible fit (not shown here) to a power law for the dynamics of sample Sr15 gives a value of $z\nu \sim 13$, which is larger than usually observed for spin glasses. However, the dynamics for this sample conform very well to the Vogel-Fulcher equation as shown in the inset of Fig. 2(b), giving a value of 5×10^{-12} sec for τ_0, 285 K for E_b/k_B and 47 K for T_0. In contrast, the dynamics of the sample Sr12.5 are described well by both the power law ($z\nu = 9.4$, $T_g = 43$ K) and the Vogel- Fulcher equation as shown in the two insets of Fig. 2(d).

To study the effect of magnetic field on the dynamics, the ac susceptibility data is collected with a superimposed dc field, H (=100, 300, 500, 1000 and 3000 Oe), while keeping the ac field amplitude at 4 Oe. Figures 3(a) and 3(b) show the in- and out-of-phase results measured at 1.7 Hz for the Sr15. The ac susceptibility data for Sr12.5 sample with superimposed dc field at 1.7 Hz is presented in the Supplemental Material [21]. The data for all measured frequencies for the Sr15 sample is shown in the Supplemental Material Fig. S3 for

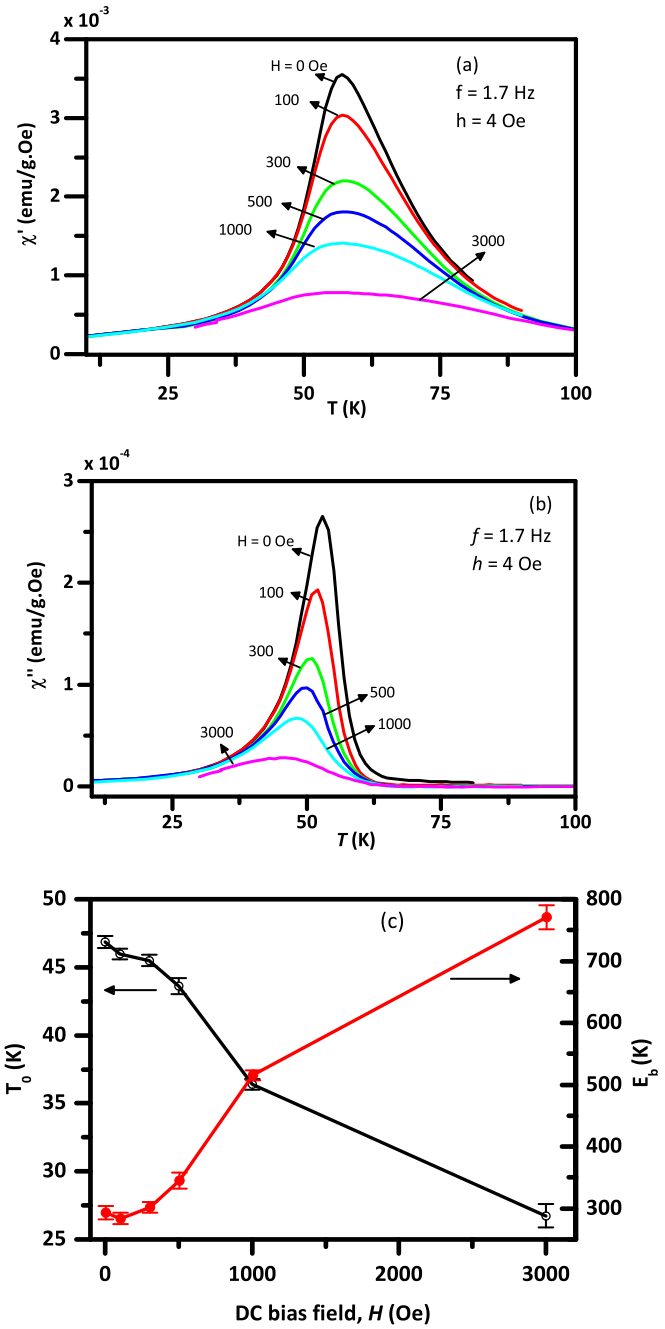

FIG. 3. Panels (a) and (b) show the real and imaginary parts of the susceptibility of crystal $La_{0.85}Sr_{0.15}CoO_3$ for various H collected with oscillating field frequency 1.7 Hz and amplitude, h, of 4 Oe. Panel (c) shows the Vogel-Fulcher fitting parameters T_0 and E_b as a function of H.

the case of 300 Oe dc bias field. Using corresponding data at all frequencies, the frequency dependent freezing temperature T_f are determined as described in the zero dc field case and the Vogel-Fulcher analysis is performed by fixing the τ_0 value to be 5×10^{-12} sec for all H values. The same τ_0 value is chosen for all H although τ_0 and E_b are coupled quantities in magnetic particle (polaron) systems. The values of T_0 and E_b obtained from the Vogel-Fulcher analysis for different H values are summarized in Fig. 3(c). The value of E_b increases with increasing H. However, the value of T_0 is seen to be decreasing with increasing H. The increasing value of E_b suggests the growth in the size of the magnetic entity with increasing H, as the anisotropy barrier energy is proportional to the volume of the magnetic entity. However, the decrease of T_0 value with increasing H is counterintuitive, as T_0 is proportional to the magnetic interaction strength between the magnetic entities. That is, in the case where there is a constant number of magnetic entities, one would expect that the interaction strength, and hence the value of T_0, should increase with increasing size of the magnetic entity. This unexpected behavior of T_0 with H can, however, be accounted for one assumes that the separation between the magnetic entities increases with H. This assumption involves a scenario where a larger number of small magnetic polarons coalesce in the presence of a magnetic field to form a smaller number of bigger polarons. Incidentally, such a scenario has been previously reported in a different context to explain overshooting hysteresis in resistivity curves of manganites [22]. It is important to mention that the Vogel-Fulcher analysis of dynamics of the other sample, Sr12.5, with a superimposed dc field, did not affect the values of T_0 and E_b as shown and described in the Supplemental Material (Fig. S3).

To determine the size of the magnetic entities that constitute the collective/glassy magnetic state of the $La_{1-x}Sr_xCoO_3$ ($x < \sim 0.18$), we have collected isothermal magnetization curves of both compounds at various temperatures above T_f and fitted the data to Langevin equation given by

$$M = nm^*\left[\coth\left(\frac{m^*H}{k_BT}\right) - \frac{k_BT}{m^*H}\right] + \chi H,$$

where n is the number of magnetic entities per mol, m^* is the moment of the magnetic entity in μ_B, χ is a field independent Curie-type magnetic susceptibility, which prevails at high temperatures and fields. As shown in Figs. 4(a) and 4(c), the magnetization data follows the Langevin equation at each temperature above T_{cusp}. The magnetization first increases nonlinearly at low magnetic fields, and linearly at larger fields, reflecting the contribution of m^* and χ, respectively. In the present case, the value of χ at 180 K (160 K) for Sr15 (Sr12.5) is determined from linear fits of the high-field M-H data. χ for lower temperatures changes according to Curie law ($\propto 1/T$). The values of n and m^* are determined as fitting parameters. The various $M(H/T)$ curves do not collapse on top of each other owing to the temperature dependence of m^*. The analyses are made under the assumption that m^* is temperature dependent, but remains nearly constant under the magnetization process at a specific temperature [23,24]. As shown in Figs. 4(a) and 4(c), the M-H data follows Langevin function for $T > T_{cusp}$ and the values of n and m^* can be determined as fitting parameters.

The value of m^* obtained as a function of temperature are shown in Figs. 4(b) and 4(d), respectively, for Sr15 and Sr12.5. The m^* values obtained in both cases indicate the presence of magnetic clusters or magnetic polarons at temperatures much higher than T_{cusp} and that the size/moment of the polarons grow with decreasing temperature as T_{cusp} is approached. The above experiment and the analysis prove that the magnetic properties of these Sr doped cobaltite crystals are characterized by magnetic polarons that may have their origin in localization of doped holes. The size of such polarons

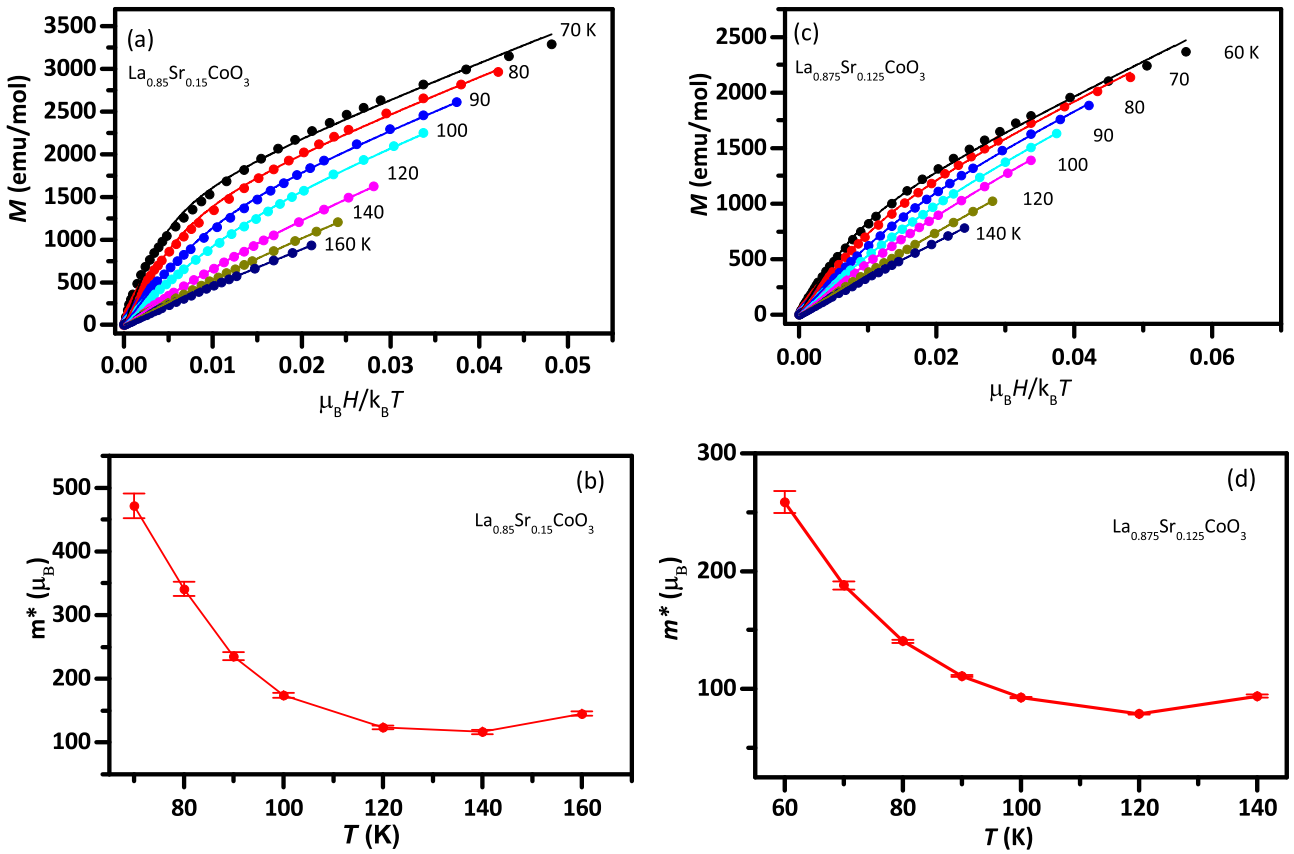

FIG. 4. The isothermal magnetization data for $T > T_{cusp}$ for samples (a) $La_{0.85}Sr_{0.15}CoO_3$ and (c) $La_{0.875}Sr_{0.125}CoO_3$. The lines are best fits using Langevin equation (see text). Panels (b) and (d) present the extracted moment value of the magnetic entity as a function of temperature for $La_{0.85}Sr_{0.15}CoO_3$ and $La_{0.875}Sr_{0.125}CoO_3$ respectively.

increases as the T_{cusp} is approached before the interpolaron interaction leads to the glassy magnetic transition at T_{cusp}. Recent investigations on Sr15 single crystals using nonlinear ac susceptibility and neutron depolarization methods also confirmed the onset of magnetic cluster growth far above the temperature at which collective behavior sets in Ref. [25]. In this aspect, SANS is a proper tool to get an idea about the size of magnetic entities [26,27].

The SANS measurement was performed on polycrystalline sample of Sr15. Macroscopic magnetization data for this polycrystalline sample is shown in the Supplemental Material Figs. S4 and S5. The net magnetic scattering intensity, after subtracting the nuclear contribution collected at different temperatures in presence of 100 Oe magnetic field is shown in Fig. 5(a). The results clearly indicate a decrease in magnetic scattering intensity with the increase in temperature up to ~120 K; above that temperature no significant magnetic contribution is observed. The nuclear scattering stemming from the powder nature of the sample has been estimated from SANS data collected at 285 K (well into the paramagnetic state) in the presence of a 20 kOe magnetic field.

Magnetic scattering intensity is mainly proportional to the square of volume of the magnetic entities and square of magnetic contrast $(\Delta\rho)^2_{mag}$, between the paramagnetic matrix and magnetic entities [28,29]. In view of that, the results in Fig. 5(a) are a clear manifestation of increase in volume of magnetic entities with decrease in temperature. We have also analyzed the SANS data by using the Lorentzian function $I(q) = I_0/(q^2 + k^2)$ to calculate the correlation length (ξ) where I_0 is constant and $\xi = 1/k$ [30,31]. The Lorentzian fits at different temperatures for zero field SANS data are shown in the Supplemental Material Fig. S6. The extracted ξ for magnetic field of 0 Oe and 100 Oe is plotted in Fig. 5(b) as a function of temperature. Below ~120 K the magnetic correlation length increases rapidly, which also has been shown in Fig. 4(b) from the analysis of $M(H, T)$ data.

In earlier reported SANS results on $La_{1-x}Sr_xCoO_3$ (for $x > 0.18$, above the percolation limit) [32] the spin correlation length, ξ sharply increases from zero at a temperature much higher than T_C and it tends to diverge as T_C is approached due to onset of long-range ordering. This increase of the correlation length occurs because of preformation of magnetic clusters at temperature much higher than T_C. Our SANS results for Sr15 do not suggest a divergence of ξ and thus the absence of long-range ordering. Instead, ξ increases below ~120 K (much higher than T_{cusp}) due to nucleation of magnetic clusters/polarons, which eventually reach the correlation length ~20–27 Å at low temperature. These results are consistent with the results obtained from the analyses of $M(H, T)$ data based on the Langevin function, the size/moment of the polaron remains finite on decreasing temperature.

In conclusion, we have found that the Sr doped $LaCoO_3$ crystals display magnetic properties characteristic of a magnetic polaron system. Our isothermal magnetization data

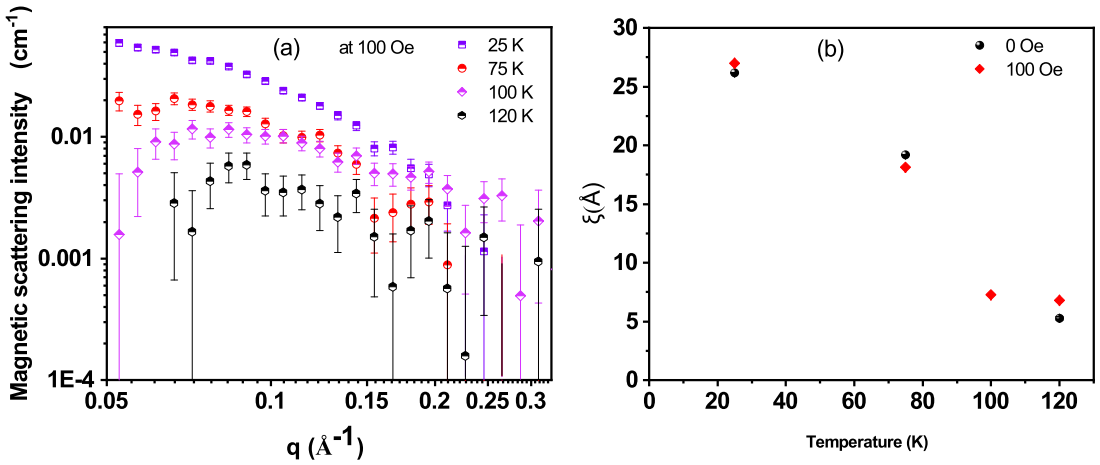

FIG. 5. (a) Magnetic scattering intensity as a function of momentum transfer (q) at different temperatures in 100 Oe magnetic field [after subtraction of 285 K (20 kOe) data] for $La_{0.85}Sr_{0.15}CoO_3$. The evolution of ξ as a function of temperature ($\leqslant$120 K) is shown in panel (b) (the error bar is smaller than the actual data point).

collected above T_{cusp} and the Langevin analysis established that the ordering magnetic entities at T_{cusp} are not atomic moments, but correspond to magnetic polarons with several hundred μ_B each. It is shown that lowering the temperature or increasing the magnetic field leads to growth of these magnetic polarons. However, the field effect on the size of magnetic polarons is not evident in case of the crystal with lower Sr doping (12.5%). The absence of the field effect in the case of the Sr12.5 can be attributed to the fact that this composition is away from the percolation threshold. The higher Sr doped compound Sr15, however, is closer to the percolation threshold (18%) and hence the polaron size shows a field dependency. Our results are consistent with the hypothesis that the SG to FM transition for systems with $x > 18\%$ Sr doping is due to the coalesce of polarons. Additionally, we also confirm the presence of magnetic polarons above T_{cusp} by analyzing a polycrystalline sample Sr15 using the SANS technique.

ACKNOWLEDGMENTS

The authors thank D. Khomskii for fruitful discussions over the experimental results. R.D. thanks Dr. S. Mukherjee for useful discussions and acknowledges IISc, India for a student fellowship. The help of A. Sundaresan and P. Yanda in obtaining the magnetic data of powder samples is gratefully acknowledged. The authors thank the Department of Science and Technology, India, as well as the Swedish Foundation for International Cooperation in Research and Higher Education (STINT) for supporting this research and ISIS neutron and muon source for the provision of beamtime RB1768009. P.A.K., R.M., and P. N. thank the Swedish Research Council (VR) and the Göran Gustafsson Foundation, Sweden for funding. R.D. also thanks the nanomission fund for supporting the visit to ISIS, UK. D.D.S. thanks the Science and Engineering Research Board, Government of India and Jamsetji Tata Trust for support of this research.

[1] S. Yamaguchi, Y. Okimoto, and Y. Tokura, Local lattice distortion during the spin-state transition, Phys. Rev. B **55**, R8666 (1997).

[2] S. Yamaguchi, Y. Okimoto, H. Taniguchi, and Y. Tokura, Spin-state transition and high-spin polarons in $LaCoO_3$, Phys. Rev. B **53**, R2926 (1996).

[3] M. Itoh, I. Natori, S. Kubota, and K. Motoya, Spin-glass behavior and magnetic phase diagram of $La_{1-x}Sr_xCoO_3$ ($0 \leqslant x \leqslant 0.5$) studied by magnetization measurements, J. Phys. Soc. Jpn. **63**, 1486 (1994).

[4] R. X. Smith, M. J. R. Hoch, W. G. Moulton, P. L. Kuhns, A. P. Reyes, G. S. Boebinger, H. Zheng, and J. F. Mitchell, Evolution of the spin-state transition with doping in $La_{1-x}Sr_xCoO_3$, Phys. Rev. B **86**, 054428 (2012).

[5] A. Podlesnyak, G. Ehlers, M. Frontzek, A. S. Sefat, A. Furrer, T. Straessle, E. Pomjakushina, K. Conder, F. Demmel, and D. I. Khomskii, Effect of carrier doping on the formation and collapse of magnetic polarons in lightly hole-doped $La_{1-x}Sr_xCoO_3$, Phys. Rev. B **83**, 134430 (2011).

[6] R. Smith, M. Hoch, P. Kuhns, W. Moulton, A. Reyes, G. Boebinger, J. Mitchell, and C. Leighton, Spin polarons in $La_{1-x}Sr_xCoO_3$ single crystals, Phys. Rev. B **78**, 092201 (2008).

[7] A. Podlesnyak, M. Russina, A. Furrer, A. Alfonsov, E. Vavilova, V. Kataev, B. Büchner, T. Strässle, E. Pomjakushina, K. Conder, and D. I. Khomskii, Spin-State Polarons in Lightly-Hole-Doped $LaCoO_3$, Phys. Rev. Lett. **101**, 247603 (2008).

[8] J. Wu, J. Lynn, C. J. Glinka, J. Burley, H. Zheng, J. F. Mitchell, and C. Leighton, Intergranular Giant Magnetoresistance in a Spontaneously Phase Separated Perovskite Oxide, Phys. Rev. Lett. **94**, 037201 (2005).

[9] C. He, S. Eisenberg, C. Jan, H. Zheng, J. F. Mitchell, and C. Leighton, Heat capacity study of magnetoelectronic phase separation in $La_{1-x}Sr_xCoO_3$ single crystals, Phys. Rev. B **80**, 214411 (2009).

[10] J. Wu, H. Zheng, J. Mitchell, and C. Leighton, Glassy transport phenomena in a phase-separated perovskite cobaltite, Phys. Rev. B **73**, 020404(R) (2006).

[11] R. X. Smith, M. J. R. Hoch, W. G. Moulton, P. L. Kuhns, A. P. Reyes, G. S. Boebinger, H. Zheng, and J. F. Mitchell, Changes in the electronic structure and spin dynamics across the metal-insulator transition in $La_{1-x}Sr_xCoO_3$, Phys. Rev. B **93**, 024204 (2016).

[12] R. Mahendiran, A. K. Raychaudhuri, A. Chainani, and D. D. Sarma, The large magnetoresistance of $La_{1-x}Sr_xCoO_3$ at low temperatures, J. Phys. Condens. Matter **7**, L561 (1995).

[13] R. Mathieu, P. Jönsson, D. N. H. Nam, and P. Nordblad, Memory and superposition in a spin glass, Phys. Rev. B **63**, 092401 (2001).

[14] M. S. Andersson, R. Mathieu, P. S. Normile, S. S. Lee, G. Singh, P. Nordblad, and J. A. De Toro, Particle size-dependent superspin glass behavior in random compacts of monodisperse maghemite nanoparticles, Mater. Res. Express **3**, 045015 (2016).

[15] M. S. Andersson, J. A. De Toro, S. S. Lee, P. S. Normile, P. Nordblad, and R. Mathieu, Effects of the individual particle relaxation time on superspin glass dynamics, Phys. Rev. B **93**, 054407 (2016).

[16] P. A. Kumar, R. Mathieu, P. Nordblad, S. Ray, O. Karis, G. Andersson, and D. D. Sarma, Reentrant Superspin Glass Phase in a $La_{0.82}Ca_{0.18}MnO_3$ Ferromagnetic Insulator, Phys. Rev. X **4**, 011037 (2014).

[17] H. Kawamura and T. Taniguchi, Spin glasses, Handb. Magn. Mater. **24**, 1 (2015).

[18] R. Mathieu and Y. Tokura, The nanoscale phase separation in hole-doped manganites, J. Phys. Soc. Jpn. **76**, 124706 (2007).

[19] R. V. Chamberlin, Mesoscopic Mean-Field Theory for Supercooled Liquids and the Glass Transition, Phys. Rev. Lett. **82**, 2520 (1999).

[20] S. Shtrikman and E. P. Wohlfarth, The theory of the Vogel-Fulcher law of spin glasses, Phys. Lett. A **85**, 467 (1981).

[21] See Supplemental Material at http://link.aps.org/supplemental/10.1103/PhysRevResearch.2.043344 for additional data on Sr12.5 sample and powder sample used for SANS study.

[22] D. Khomskii and L. Khomskii, Fine mist versus large droplets in phase separated manganites, Phys. Rev. B **67**, 052406 (2003).

[23] G. H. McCabe, T. Fries, M. T. Liu, Y. Shapira, L. R. Ram-Mohan, R. Kershaw, A. Wold, C. Fau, M. Averous, and E. J. McNiff, Bound magnetic polarons in p -type $Cu_2Mn_{0.9}Zn_{0.1}SnS_4$, Phys. Rev. B **56**, 6673 (1997).

[24] P. Nordblad, L. Lundgren, and O. Beckman, Magnetic cluster effects in $FeSi_{1-x}Ge_x$, Phys. Scr. **28**, 246 (1983).

[25] A. V. Lazuta, V. A. Ryzhov, V. V. Runov, V. P. Khavronin, and V. V. Deriglazov, Temperature evolution of superparamagnetic clusters in single-crystal $La_{0.85}Sr_{0.15}CoO_3$ characterized by nonlinear magnetic ac response and neutron depolarization, Phys. Rev. B **92**, 014404 (2015).

[26] D. Alba Venero, S. E. Rogers, S. Langridge, J. Alonso, M. L. Fdez-Gubieda, A. Svalov, and L. Fernández Barquín, Magnetic nanoscopic correlations in the crossover between a superspin glass and a superferromagnet, J. Appl. Phys. **119**, 143902 (2016).

[27] C. Bellouard, I. Mirebeau, and M. Hennion, Magnetic correlations of fine ferromagnetic particles studied by small-angle neutron scattering, Phys. Rev. B **53**, 5570 (1996).

[28] A. Michels, Magnetic small-angle neutron scattering of bulk ferromagnets, J. Phys.: Condens. Matter **26**, 383201 (2014).

[29] G. Biotteau, M. Hennion, R. Moussa, J. Rodriguez-Carvajal, L. Pinsard, A. Revcolevschi, Y. M. Mukovskii, and D. Shulyatev, Approach to the metal-insulator transition in $La_{1-x}Ca_xMnO_3$ $(0 \leqslant x \leqslant 0.2)$: magnetic inhomogeneity and spin-wave anomaly, Phys. Rev. B **64**, 104421 (2001).

[30] J. M. De Teresa, M. R. Ibarra, P. A. Algarabel, C. Ritter, C. Marquina, J. Blasco, J. García, A. del Moral, and Z. Arnold, Evidence for magnetic polarons in the magnetoresistive perovskites, Nature (London) **386**, 256 (1997).

[31] C. Magen, P. A. Algarabel, L. Morellon, J. P. Araújo, C. Ritter, M. R. Ibarra, A. M. Pereira, and J. B. Sousa, Observation of a Griffiths-Like Phase in the Magnetocaloric Compound $Tb_5Si_2Ge_2$, Phys. Rev. Lett. **96**, 167201 (2006).

[32] C. He, M. A. Torija, J. Wu, J. W. Lynn, H. Zheng, J. F. Mitchell, and C. Leighton, Non-Griffiths-like clustered phase above the curie temperature of the doped perovskite cobaltite $La_{1-x}Sr_xCoO_3$, Phys. Rev. B **76**, 014401 (2007).